Ocean Systems Engineering, *Vol. 12, No. 1 (2022) 1-22*
https://doi.org/10.12989/ose.2022.12.1.001

SCFs in offshore two-planar tubular TT-joints reinforced with internal ring stiffeners

Hamid Ahmadi*[1,2] and Hossein Imani[1]

[1]*Faculty of Civil Engineering, University of Tabriz, Tabriz 5166616471, Iran*
[2]*Center of Excellence in Hydroinformatics, Faculty of Civil Engineering, University of Tabriz, Tabriz, Iran*

(Received April 8, 2021, Revised December 29, 2021, Accepted January 13, 2022)

Abstract. The majority of tubular joints commonly found in offshore jacket structures are multi-planar. Investigating the effect of loaded out-of-plane braces on the values of the stress concentration factor (SCF) in offshore tubular joints has been the objective of numerous research works. However, due to the diversity of joint types and loading conditions, a number of quite important cases still exist that have not been studied thoroughly. Among them are internally ring-stiffened two-planar TT-joints subjected to axial loading. In the present research, data extracted from the stress analysis of 243 finite element (FE) models, verified against available numerical and experimental data, was used to study the effects of geometrical parameters on the chord-side SCFs in two-planar tubular TT-joints reinforced with internal ring stiffeners subjected to two types of axial loading. Parametric FE study was followed by a set of nonlinear regression analyses to develop six new SCF parametric equations for the fatigue analysis and design of axially-loaded two-planar TT-joints reinforced with internal ring stiffeners.

Keywords: fatigue; internal ring stiffener; offshore jacket structure; stress concentration factor (SCF); two-planar tubular TT-joint

1. Introduction

The primary structural part of an offshore jacket-type platform, commonly used for the production of oil and gas from hydrocarbon reservoirs below the seabed (Fig. 1(a)), is fabricated from tubular members by welding one end of the branch member, i.e. brace, to the undisturbed surface of the main member, i.e., chord, resulting in what is known as a tubular joint (Fig. 1(b)). The static and fatigue strength of tubular joints are the governing factors in the design of jacket structures.

Tubular joints must be properly dimensioned during the design stage so that they perform satisfactorily in service and achieve a reasonable balance between the project cost and risk of failure. If the capacity of a joint is found to be inadequate during the design stage, it can be enhanced by welding ring stiffeners onto the inner surface of the chord (Fig. 1(c)) as this is an efficient method to reduce the stress concentration, increase the load-carrying capacity and fatigue life of the joint, and avoid the attraction of additional wave forces. The use of internally ring-stiffened tubular joints to enhance the static capacity and to reduce the stress concentration was common practice in the

*Corresponding author, E-mail: h-ahmadi@tabrizu.ac.ir

http://www.techno-press.org/?journal=ose&subpage=7 ISSN: 2093-6702 (Print), 2093-677X (Online)

design of fixed steel platforms up to the late eighties. The increase in crane lifting capacity for platform launching, larger fabrication limits and the recognition of the difficulties in detecting the in-service internal cracks mean that the internal ring-stiffeners are not common in modern design. Nevertheless, guidance on fatigue performance is still needed for the purposes of structural assessment of older platforms. It is estimated that there are at least 2000 ring-stiffened joints in the North Sea alone (Wimpey Offshore, 1991). None of the major offshore design codes, such as API RP 2A (2007) and HSE (1995), provides any substantial quantitative recommendations on fatigue strength requirements for internally ring-stiffened joints. This is due partly to the vast variety of possible stiffening arrangements and partly to the dearth of information available on such joints in research literature. There is, therefore, a need for further research so that more detailed guidelines on fatigue strength estimation of internally ring-stiffened tubular joints can be formulated, which is the incentive of the present work.

Significant stress concentrations at the vicinity of the welds are considerably detrimental to the fatigue performance of the joints. Hence, it is important to accurately determine the magnitude of stress concentration and to reduce it to a reasonable level. In the design practice, a parameter called the stress concentration factor (SCF) is used to evaluate the magnitude of the stress concentration. The SCF, defined as the ratio of the local surface stress at the brace-to-chord intersection to the nominal stress in the brace, exhibits considerable scatter depending on the joint geometry, loading type, weld size and type, and the considered position for the SCF calculation around the weld profile. Under any specific loading condition, the SCF value along the weld toe of a tubular joint is mainly determined by the joint geometry. To study the behavior of tubular joints and to easily relate this behavior to the geometrical characteristics of the joint, a set of dimensionless geometrical parameters has been defined. Fig. 1(c) depicts an internally ring-stiffened two-planar tubular TT-joint with the geometrical parameters τ, γ, β, η, α, and α_B where D and d are the diameters of the chord and brace, respectively; L and l are the lengths of those members, respectively; and T, t, and w_s are the chord thickness, the brace thickness, and the stiffener width, respectively. Critical positions along the weld toe of the brace-to-chord intersection for the calculation of SCFs in a tubular joint, i.e., saddle and crown, have been shown in Fig. 1(b) and 1(c).

Over the past fifty years, significant effort has been devoted to the study of SCFs in various uniplanar tubular joints (i.e., joints where the axes of the chord and brace members lay on the same plane). As a result, many parametric design formulas in terms of the joint's geometrical parameters have been proposed providing SCF values at certain positions adjacent to the weld for several loading conditions. Multi-planar joints (i.e., joints where the axes of the chord and all brace members do not lay on the same plane) are an intrinsic feature of offshore tubular structures. The multi-planarity effect might play an important role in the stress distribution along the brace-to-chord intersection. Thus for multi-planar connections, the parametric formulas of simple uniplanar tubular joints may not be applicable for the SCF prediction; since such formulas may lead to highly over- or under-predicting results. Nevertheless, for multi-planar joints which cover the majority of practical applications, much fewer investigations have been reported due to the complexity and high cost involved.

In the present paper, results of a numerical investigation on the SCFs in two-planar tubular TT-joints, also called multi-planar DT-joints, reinforced with internal ring stiffeners are presented and discussed. In this research program, a set of parametric finite element (FE) stress analyses was carried out on 243 internally ring-stiffened tubular TT-joint models subjected to two types of axial loading (Fig. 2). Analysis results were used to present general remarks on the effects of geometrical parameters including τ (brace-to-chord thickness ratio), γ (chord wall slenderness ratio), β (brace-

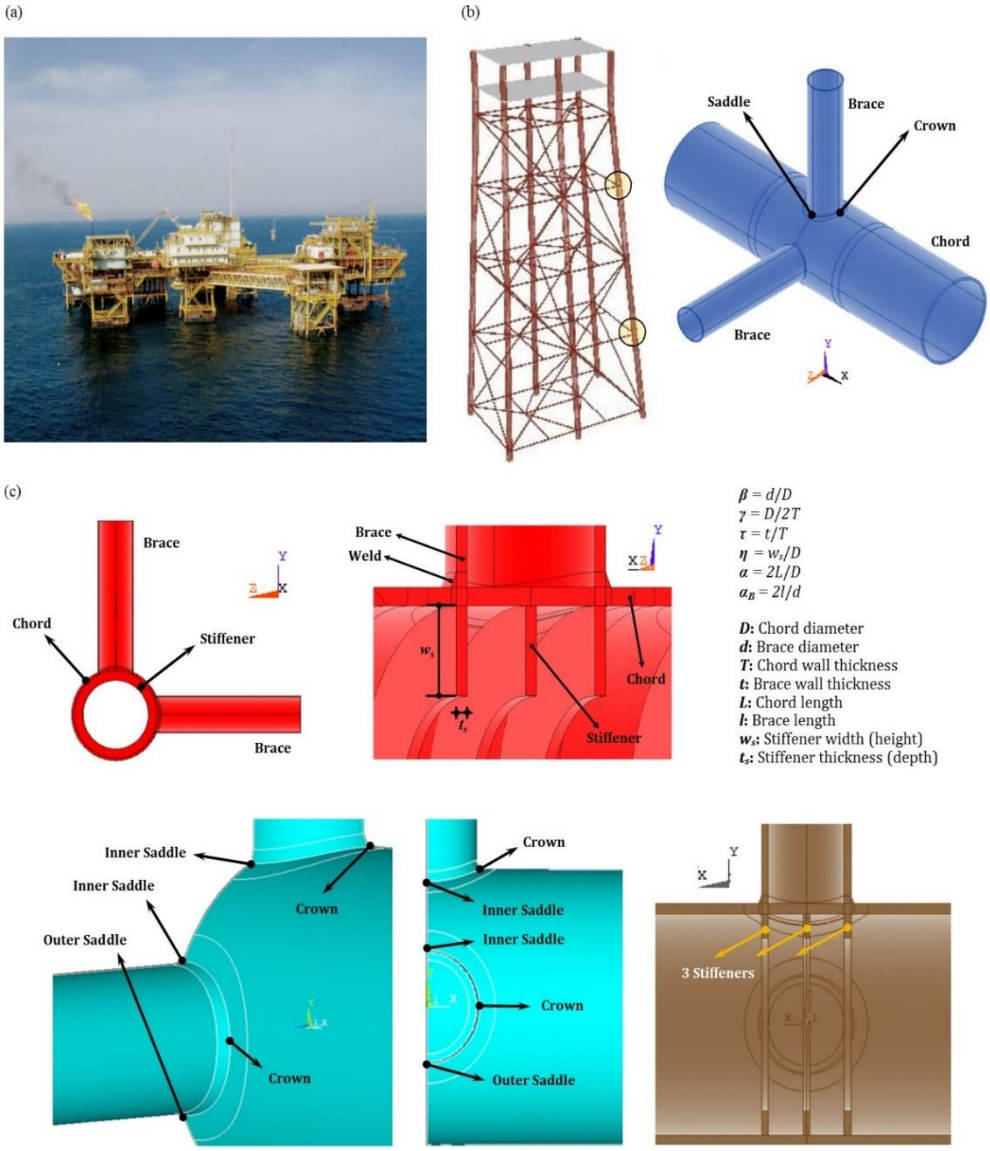

Fig. 1 (a) A jacket-type offshore platform, (b) A two-planar tubular TT-joint reinforced with internal ring stiffeners and (c) Geometrical notation for an internally ring-stiffened two-planar TT-joint

to-chord diameter ratio), α (chord length-to-radius ratio), and η (ring width to chord diameter ratio) on the SCFs at the saddle and crown positions. Based on the results of internally ring-stiffened TT-joint FE models, verified against experimental and numerical data, an SCF database was prepared.

Then, a new set of SCF parametric equations was established, based on nonlinear regression analyses, for the fatigue analysis and design of two-planar tubular TT-joints reinforced with internal ring stiffeners subjected to axial loading. The reliability of proposed equations was evaluated according to the acceptance criteria recommended by the UK DoE (1983).

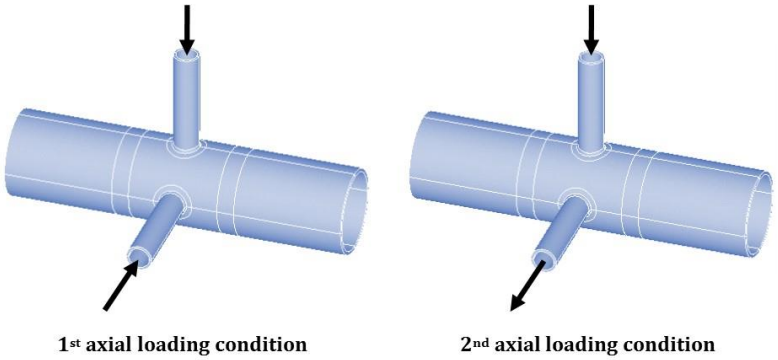

Fig. 2 Studied axial loading conditions

2. Literature review

2.1 Study of SCFs in unreinforced tubular joints

2.1.1 Determination of SCFs in uniplanar connections

For the study of SCFs in various uniplanar tubular joints, the reader is referred to Kuang *et al.* (1975), Efthymiou (1988), Hellier *et al.* (1990), UK HSE OTH 354 (1997), and Karamanos *et al.* (2000) for the SCF calculation at the saddle and crown positions of simple uniplanar T-, Y-, X-, K-, and KT-joints; and Gho and Gao (2004), Gao (2006), Gao *et al.* (2007), and Yang *et al.* (2015) for the SCF determination in overlapped uniplanar joints, among others.

For the study of SCF distribution along the weld toe in uniplanar tubular joints, the reader is referred for example to Morgan and Lee (1998a, b) for K-joints; Chang and Dover (1999a, b) for T-, Y-, X-, and DT-joints; Shao (2004b, 2007) and Shao *et al.* (2009) for T- and K-joints; Lotfollahi-Yaghin and Ahmadi (2010), Ahmadi *et al*. (2011c), and Lotfollahi-Yaghin and Ahmadi (2011) for KT- and DKT-joints; and Liu *et al.* (2015) for T-joints.

2.1.2 Determination of SCFs in multi-planar connections

For the SCF studies in multi-planar joints, the reader is referred to Karamanos *et al*. (1999) and Chiew *et al*. (2000) for the SCF calculation in XX-joints; Wingerde *et al*. (2001) for the SCF determination in KK-joints; Karamanos et al. (2002) for the study of SCFs in DT-joints; Chiew *et al.* (1999) for the study of SCFs in XT-joints; Ahmadi *et al*. (2011a, 2012a), Ahmadi and Lotfollahi-Yaghin (2012b), and Ahmadi and Zavvar (2016) for the investigation of SCFs in multi-planar KT-joints under axial loads; and Ahmadi and Kouhi (2020) for the SCF determination in unreinforced XT-joints subjected to out-of-plane bending (OPB) moment loadings, among others.

2.2 Study of SCFs in reinforced tubular joints

2.2.1 Determination of SCFs in uniplanar connections

For the SCF calculation at saddle and crown positions of stiffened tubular joints, the reader is referred for example to Nwosu *et al.* (1995) for ring-stiffened T-joints; Hoon *et al*. (2001) for doubler-plate reinforced T-joints; Myers *et al.* (2001) for rack-plate reinforced joints; Ahmadi and

Lotfollahi-Yaghin (2015) and Ahmadi and Zavvar (2015) for ring-stiffened KT-joints subjected to in-plane bending (IPB) moment and OPB moment loadings; and Xu *et al*. (2015) for concrete-filled joints.

Ahmadi *et al*. (2012b, 2013) investigated the SCF distribution along the weld toe of central and outer braces in tubular KT-joints reinforced with internal ring stiffeners and proposed a set of parametric equations to calculate the SCFs along the brace-to-chord intersection in internally ring-stiffened KT-joints subjected to axial loading.

2.2.2 Determination of SCFs in multi-planar connections

Woghiren and Brennan (2009) developed a set of parametric equations to predict the SCFs at critical positions along the brace-to-chord intersection in two-planar tubular KK-joints reinforced with rack plates.

2.3 Other behavioral and SCF-related studies in various tubular joints

For other behavioral and SCF-related investigations such as probabilistic studies, strength estimations, and local flexibility assessments, the reader is referred for example to Ahmadi *et al*. (2011b), Gaspar *et al.* (2011), Guarracino (2011), Ahmadi and Lotfollahi-Yaghin (2012a, 2013), Ahmadi et al. (2015, 2016), Ahmadi (2016), Ahmadi and Mousavi Nejad Benam (2017), Asgarian *et al.* (2014), and Prashob *et al*. (2018).

2.4 Concluding remarks

It can be clearly concluded from Sect. 2.1–2.3 that, over the past five decades, significant effort has been devoted to the study of SCFs in various unstiffened tubular joints including both uniplanar and multi-planar connections. Albeit, the majority of these studies are on uniplanar joints.

However, the study of SCFs in stiffened joints is rather limited. It is also evident that in the case of stiffened joints, almost all of available research reports are on the SCFs in uniplanar connections and the studies on the SCFs in multi-planar stiffened joints are quite rare.

Despite the use of two-planar tubular TT-joints reinforced with internal ring stiffeners in the design of offshore jacket-type structures, the SCFs in internally ring-stiffened TT-joints have not been investigated and no design equation is currently available to determine the weld-toe SCFs at the saddle and crown positions in this type of joint.

3. FE modeling

3.1 Modeling of ring stiffeners

The simplest and most accurate way to model the interaction between the chord and the stiffener is to glue their volumes during the geometrical modeling by which the generated mesh for these volumes will be automatically merged together. However, this straight-forward method is not applicable in the present study. The reason is that gluing the volumes of the chord and the stiffener during the geometrical modeling will produce serious problems in generating a high-quality mesh around the brace-to-chord intersection. Consequently, due to the poor quality and irregularity of the generated mesh along the brace-to-chord intersection, it is almost impossible to accurately determine

the extrapolated SCFs along the intersection based on the stresses perpendicular to the weld toe. In such situation, only the SCF at the saddle position may be extracted accurately. In the present study, in order to resolve this problem, the chord and stiffener were meshed separately and then the ANSYS contact capability was used to define the interaction between them. In problems involving contact between two boundaries, one of the boundaries in conventionally established as the "target" surface and the other as the "contact" surface. In this study, the outer surfaces of the rings were introduced as the target surface and inner surface of the chord was established as the contact surface. Flexible-to-flexible surface-to-surface contact elements were used to simulate the interaction. Augmented Lagrange method was used as the contact algorithm and the behavior of the contact surface was defined to be always bonded. Contact was set to be detected on Gauss points and be automatically adjusted to close the gap and reduce the penetration. For detailed information on selecting suitable contact options and settings, for example guidelines for designating the "target" and "contact" surfaces, the reader is referred to ANSYS Contact Technology Guide (Swanson Analysis Systems Inc., 2009).

For axial loading, the most effective position for ring stiffeners has been found to be the middle half of the plug (Nwosu *et al.* 1995). However, the use of a single stiffener at the saddle position is not recommended since it produces a region of high local stiffness through which a high proportion of the load is transferred causing high SCFs on the chord and brace side (Myers *et al.* 2001). Hence, as shown in Fig. 1(c), three ring stiffeners were used in all models: One at the saddle position and the other two at the crown positions. In order to avoid high stress concentrations in the stiffener, thickness of the stiffener should not be less than the brace wall thickness. On the other hand, according to Nwosu *et al.* (1995), the inertia moment of the stiffener, in the radial direction of the chord, is the main factor in controlling the SCFs. This result suggests that using thin tall stiffeners can lead to optimum SCF values. Hence, the stiffener thickness was designated to be equal to the brace wall thickness in all models of the present study.

3.2 Simulation of the weld profile

Accurate modeling of the weld profile is one of the most critical factors affecting the accuracy of SCF results. Therefore, the weld sizes must be carefully included in the FE modeling. A number of research works has been carried out on the study of the weld effect. For example, the reader is referred to Lee and Wilmshurst (1995), Cao *et al*. (1997), and Lee (1999), among others. It was found that the fatigue strength of the joint can be underestimated by 20% compared to the experimental data without considering the weld (Shao 2004a).

In the present study, the welding size along the brace-to-chord intersection satisfies the AWS D 1.1 (2002) specifications. However, it should be noted that attempts to produce an improved as-welded profile often result in over-welding. Consequently, the actual weld size, typical of yard practice, is usually different from the nominal weld size recommended by AWS D 1.1 (2002). For the correction of SCFs to consider the actual position of the weld toe, the reader is advised to follow the recommendations of Section C 5.3.2(a) of API RP 2A (2007).

Considering the effect of possible weld defects, it should be noted that for fatigue design purposes, the hot-spot stress (HSS) method has been quite efficient and popular. According to this method, the nominal stress at the joint members is multiplied by an appropriate SCF to provide the HSS at a certain location. HSSs are calculated at various positions around the weld and the maximum HSS range (S) is determined. Then, the fatigue life of the joint is estimated through an appropriate S–N fatigue curve, N being the number of load cycles. The HSS range concept places different structural

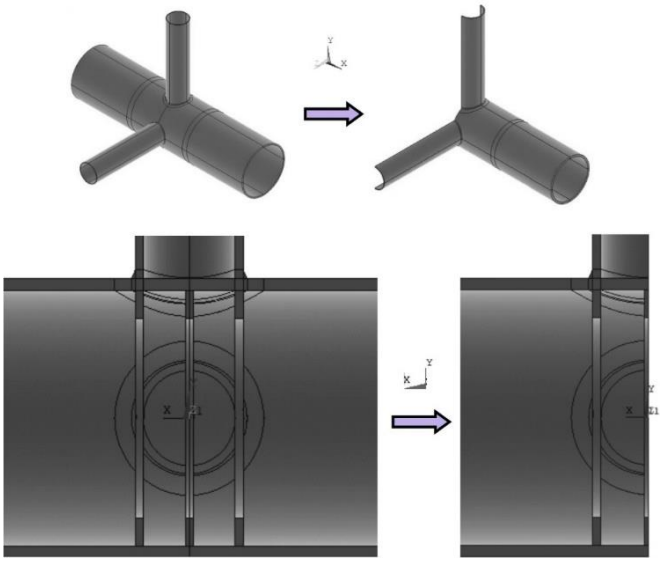

Fig. 3 One quarter of the entire internally ring-stiffened two-planar TT-joint that is required to be modeled under studied axial loading conditions

geometries on a common basis, enabling them to be treated using a single *S–N* curve. The basis of this concept is to capture a stress (or strain) in the proximity of the weld toes, which characterizes the fatigue life of the joint, but excludes the very local microscopic effects like the sharp notch, undercut and crack-like defects at the weld toe. These local weld notch effects are included in the *S–N* curve.

The dihedral angle (ψ) which is an important parameter in determining the weld thickness is defined as the angle between the chord and brace surface along the intersection curve. The dihedral angle at the two typically important positions along the weld toe, i.e., saddle and crown, equals to π–$\cos^{-1}(\beta)$ and $\pi/2$, respectively. Details of weld profile modeling according to AWS D 1.1 (2002) have been presented by Ahmadi *et al.* (2012a).

3.3 Boundary conditions

In offshore structures, the chord end fixity conditions of tubular joints may range from almost fixed to almost pinned with generally being closer to almost fixed (Efthymiou 1988). In practice, the value of the parameter α in over 60% of tubular joints is in excess of 20 and is bigger than 40 in 35% of the joints (Smedley and Fisher 1991). Changing the end restraint from fixed to pinned results in a maximum increase of 15% in the SCF at the crown position for joints with $\alpha = 6$, and this increase reduces to only 8% for $\alpha = 8$ (Morgan and Lee 1998b). In the view of the fact that the effect of chord end restraints is only significant for joints with $\alpha < 8$ and high β and γ values, which do not commonly occur in practice, both chord ends were assumed to be fixed, with the corresponding nodes restrained. Due to the symmetry in geometry and loading of the joint, only half of the entire internally ring-stiffened tubular TT-joint is required to be modeled in order to reduce the computational time (Fig. 3). Appropriate symmetric boundary conditions were defined for the nodes located on the symmetry planes.

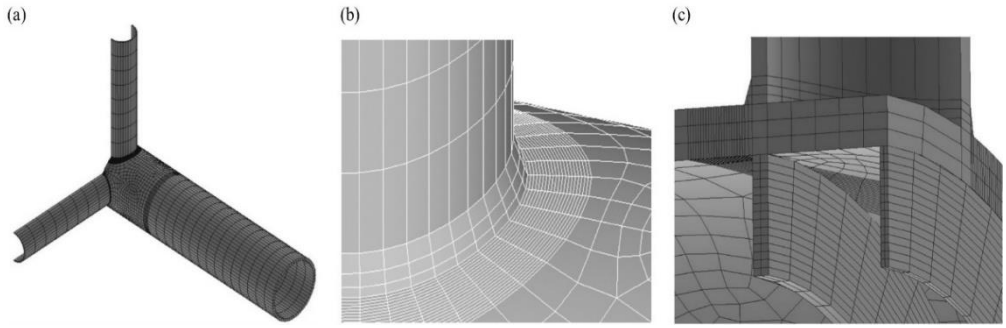

Fig. 4 Generated mesh by the sub-zone scheme: (a) Half of the joint under the axial loading condition, (b) Region adjacent to the brace-to-chord intersection, (c) Internal ring stiffeners

3.4 Mesh generation

In the present study, ANSYS element SOLID95 was used to model the chord, braces, rings, and weld profiles. This element type has compatible displacements and is well-suited to model curved boundaries. It is defined by 20 nodes having three degrees of freedom per node and may have any spatial orientation. Using this type of 3-D brick elements, the weld profile can be modeled as a sharp notch. This method will produce more accurate and detailed stress distribution near the intersection in comparison with a shell analysis.

To guarantee the mesh quality, a sub-zone mesh generation scheme was used during the FE modeling. The entire structure was divided to several zones according to computational requirements. The mesh of each zone was generated separately and then the mesh of the entire joint was produced by merging the meshes of all the sub-zones. This scheme can feasibly control the mesh quantity and quality and avoid badly distorted elements. The mesh generated by this procedure for an internally ring-stiffened tubular TT-joint is shown in Fig. 4.

As mentioned earlier, in order to determine the SCF, the stress at the weld toe should be divided by the nominal stress of the loaded brace. The stresses perpendicular to the weld toe at the extrapolation points are required to be calculated in order to determine the stress at the weld toe position. To extract and extrapolate the stresses perpendicular to the weld toe, as shown in Figs. 4 and 5(b), the region between the weld toe and the second extrapolation point was meshed finely in such a way that each extrapolation point was placed between two nodes located in its immediate vicinity. These nodes are located on the element-generated paths which are perpendicular to the weld toe.

In order to verify the convergence of FE results, convergence test with different mesh densities was conducted before generating the 243 FE models for the parametric study.

3.5 Analysis settings and SCF calculation

Static analysis of the linearly elastic type is suitable to determine the SCFs in tubular joints (N'Diaye *et al.* 2007). The Young's modulus and Poisson's ratio were taken to be 207 GPa and 0.3, respectively.

The weld-toe SCF is defined as

$$\text{SCF}=\sigma_{\perp W}/\sigma_n \tag{1}$$

In Eq. (1), σ_n is the nominal stress of the axially loaded brace which is calculated as follows

$$\sigma_n = \frac{4F_a}{\pi\left[d^2 - (d-2t)^2\right]} \tag{2}$$

where F_a is the applied axial force; and d and t are brace diameter and thickness, respectively.

To calculate the SCF, the stress at the weld toe position should be extracted from the stress field outside the region influenced by the local weld toe geometry. The location from which the stresses have to be extrapolated, *extrapolation region*, depends on the dimensions of the joint and on the position along the intersection.

According to the linear extrapolation method recommended by IIW XV-E (1999), the first extrapolation point must be at a distance of $0.4T$ from the weld toe, and the second point should lie at $1.0T$ further from the first point (Fig. 5(a)). In Eq. (1), $\sigma_{\perp W}$ is the extrapolated stress at the weld toe position which is perpendicular to the weld toe and is calculated by the following equation

$$\sigma_{\perp W} = 1.4\sigma_{\perp E1} - 0.4\sigma_{\perp E2} \tag{3}$$

where $\sigma_{\perp E1}$ and $\sigma_{\perp E2}$ are the stresses at the first and second extrapolation points along the direction perpendicular to the weld toe, respectively.

The stress at an extrapolation point is obtained as follows

$$\sigma_{\perp E} = \frac{\sigma_{\perp N1} - \sigma_{\perp N2}}{\delta_1 - \delta_2}(\Delta - \delta_2) + \sigma_{\perp N2} \tag{4}$$

where $\sigma_{\perp Ni}$ (i = 1 and 2) is the nodal stress at the immediate vicinity of the extrapolation point along the direction perpendicular to the weld toe at the saddle position (Eq. (5)); δ_i (i = 1 and 2) is the distance between the weld toe and the considered node inside the extrapolation region (Eq. (6)); and Δ equals to $0.4T$ and $1.4T$ for the first and second extrapolation points, respectively (Fig. 5(b)).

$$\sigma_{\perp N} = \sigma_x l_1^2 + \sigma_y m_1^2 + \sigma_z n_1^2 + 2\left(\tau_{xy} l_1 m_1 + \tau_{yz} m_1 n_1 + \tau_{zx} n_1 l_1\right) \tag{5}$$

$$\delta = \sqrt{(x_w - x_n)^2 + (y_w - y_n)^2 + (z_w - z_n)^2} \tag{6}$$

In Eq. (5), σ_a and τ_{ab} ($a, b = x, y, z$) are components of the stress tensor which can be extracted from ANSYS analysis results; and l_1, m_1, and n_1 are transformation components defined as:

$$l_1 = \cos(X_\perp, x); \quad m_1 = \cos(X_\perp, y); \quad n_1 = \cos(X_\perp, z) \tag{7}$$

where $X_\perp$ is the direction perpendicular to the weld toe; and x, y, and z are axes of the global coordinate system (Fig. 5(b)). These components can be calculated as below:

$$l_1 = (x_w - x_n)/\delta; \quad m_1 = (y_w - y_n)/\delta; \quad n_1 = (z_w - z_n)/\delta \tag{8}$$

where (x_n, y_n, z_n) and (x_w, y_w, z_w) are global coordinates of the considered node inside the extrapolation region and its corresponding node at the weld toe position, respectively.

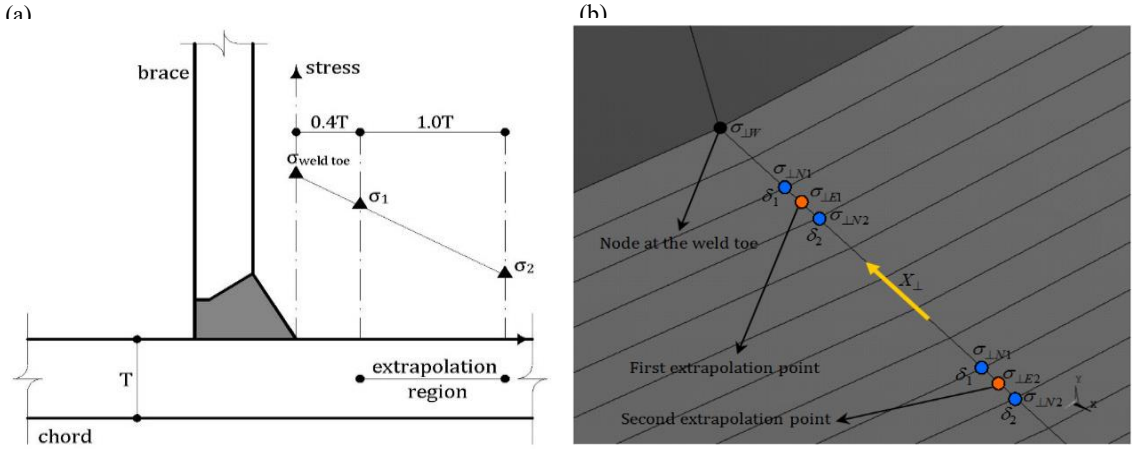

Fig. 5 (a) Extrapolation method according to IIW XV-E (1999) and (b) Required interpolations and extrapolations to extract the HSS value at the weld toe

At the saddle and crown positions, Eq. (5) is simplified as

$$\sigma_{\perp N} = \sigma_y m_1^2 + \sigma_z n_1^2 + 2\tau_{yz} m_1 n_1 \quad \text{(Saddle)}; \quad \sigma_{\perp N} = \sigma_x \quad \text{(Crown)} \tag{9}$$

In order to facilitate the SCF calculation, above formulation was implemented in a *macro* developed by the ANSYS Parametric Design Language (APDL). The input data required to be provided by the user of the macro are the node number at the weld toe, the chord thickness, and the numbers of the nodes inside the extrapolation region. These nodes can be introduced using the Graphic user interface (GUI).

3.6 FE model verification

As far the authors can tell, there is no experimental/numerical data available in the literature on the SCFs in internally ring-stiffened two-planar tubular TT-joints that are studied in the present research. However, a set of related experimental and numerical data is available that can be used for the verification of present FE models.

3.6.1 HSE OTH 354 (1997) experimental data

Experimental data on the SCFs of uniplanar T-joints published in HSE OTH 354 (1997) was used to validate the present FE models. In order to do so, an FE model was generated for a T-joint having the same geometrical characteristics as the T39 specimen (Table 1) and the model was analyzed subjected to brace axial loading (Fig. 6(a)). The method of geometrical modeling (introducing the chord, brace, and weld profile), the mesh generation procedure (including the selection of element type and size), load application, analysis method, and the method of SCF extraction are identical for the T-joint validating model and the TT-joint models used for the parametric study. Hence, the verification of SCF values derived from validating FE model with the experimental data from HSE OTH 354 (1997) lends some support to the validity of SCF values derived from the FE models of present paper. Results of verification process are presented in Table 2. It can be seen that there is a

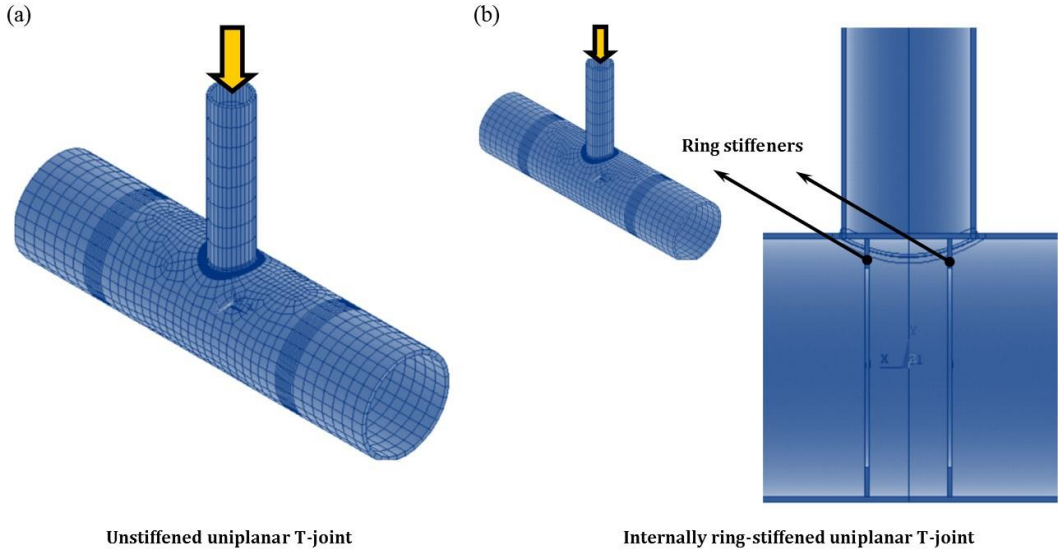

Fig. 6 (a) Validating FE model generated for the comparison of the results with HSE OTH 354 (1997) experimental measurements and (b) Validating FE model generated to compare the results with Nwosu *et al.* (1995) numerical data

Table 1 Properties of uniplanar tubular T-joint used for the verification of present FE model

Joint ID (HSE OTH 354, 1997)	Material	Loading type	D (mm)	τ	β	γ	α
T39	Steel	Axial	457	0.4	0.25	14.3	10.2

Table 2 Results of the FE model verification based on HSE OTH 354 (1997) experimental data

Position	SCF		Difference
	Present FE model	Experimental data (HSE OTH 354, 1997)	
Crown	2.41	2.40	0.41%
Saddle	4.81	4.20	12.68%

good agreement between the results of present FE model and HSE OTH 354 (1997) experimental data. The average and maximum differences between the results are less than 7% and 13%, respectively. Hence, generated FE models can be considered to be accurate enough to provide valid results.

3.6.2 Numerical and experimental results of Nwosu et al. (1995)

Nwosu *et al.* (1995) presented a set of numerical and experimental results for the estimation of SCFs in axially loaded uniplanar tubular T-joints reinforced with internal ring stiffeners (Fig. 6(b)). This data was used in the present study to validate the generated FE models. In order to do so, an FE model was generated for an internally ring-stiffened T-joint having the same geometrical characteristics as an FE model generated by Nwosu *et al*. (1995) and the model was analyzed

Table 3 Properties of internally ring-stiffened T-joint used for the verification of present FE model

Loading type	D (mm)	d (mm)	T (mm)	t (mm)	L (mm)	l (mm)	w_s (mm)	t_s (mm)	Δ_s* (mm)
Axial	914	457	16	16	2458	1828	100	16	266

* Δ_s: Distance between stiffeners

Table 4 Results of the FE model verification based on experimental and numerical data provided by Nwosu *et al.* (1995)

Position	SCF			(1) & (2) difference	(1) & (3) difference
	1. Present FE model	2. National Engineering Lab (NEL) experimental data (Nwosu *et al*. 1995)	3. Nwosu *et al*. (1995) numerical results		
Saddle	8.30	7.30	7.30	12.05%	12.05%
Crown	3.71	4.43	4.00	16.25%	7.25%

subjected to axial loading (Table 3). Geometrical modeling process, the mesh generation procedure, analysis method, and the method of SCF extraction are identical for the ring-stiffened T-joint validating model and the ring-stiffened TT-joint models used for the parametric study. Hence, the verification of SCF values derived from validating FE model with Nwosu *et al*. (1995) numerical and experimental data lends some support to the validity of SCF values derived from the FE models used for the parametric study of present research. Results of verification process are presented in Table 4. It can be seen that there is a good agreement between the results of present FE model and the data provided by Nwosu *et al*. (1995). The maximum difference between the results of present FE model and Nwosu et al.'s experimental and numerical data are about 16% and 12%, respectively. Hence, generated FE models can be considered to be accurate enough to provide valid results.

4. Effects of geometrical parameters on the SCFs

In order to study the SCFs in two-planar tubular TT-joints reinforced with internal ring stiffeners subjected to two types of axial loading (Fig. 2), 243 models were generated and analyzed using the FE software, ANSYS. The objective was to investigate the effects of non-dimensional geometrical parameters on the chord-side SCFs at the saddle and crown positions.

Different values assigned for parameters β, γ, τ, α, and η have been presented in Table 5. These values cover the practical ranges of the dimensionless parameters typically found in tubular joints of offshore jacket structures. The brace length has no effect on SCFs when the parameter α_B is greater than a critical value (Chang and Dover 1999a). In the present study, in order to avoid the effect of short brace length, a realistic value of $\alpha_B = 8$ was assigned to all joints. The 243 generated models span the following ranges of the geometric parameters

$$\begin{aligned} 0.3 \le \beta \le 0.5 \\ 12 \le \gamma \le 24 \\ 0.4 \le \tau \le 1.0 \\ 8 \le \alpha \le 24 \\ 0.1 \le \eta \le 0.2 \end{aligned} \tag{10}$$

Table 5 Values assigned to each dimensionless parameter

Parameter	Definition	Value(s)
β	d	0.3, 0.4, 0.5
γ	D	12, 18, 24
τ	t	0.4, 0.7, 1.0
η	w_s/D	0.1, 0.15, 0.2
α	L	8, 16, 24
α_B	l	8

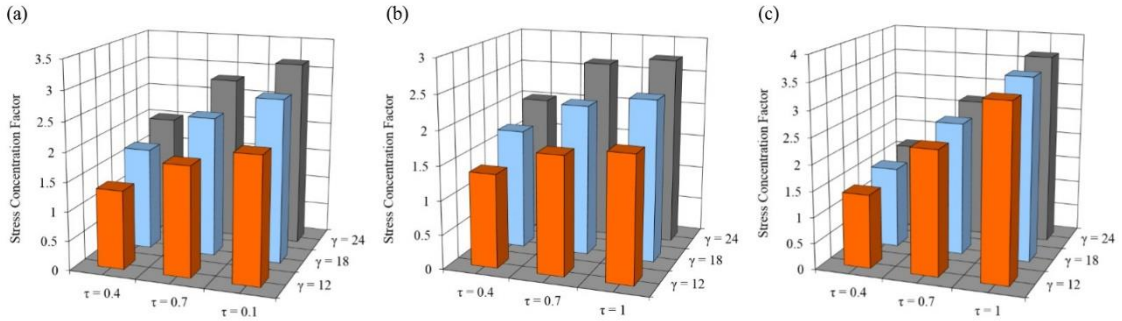

Fig. 7 The effect of the τ on the SCFs at different positions (β = 0.4, α = 16, η = 0.15; 1st axial loading condition): (a) Inner saddle, (b) Outer saddle and (c) Crown

The parameter τ is the ratio of brace thickness to chord thickness and the γ is the ratio of radius to thickness of the chord. Hence, the increase of the τ in models having constant value of the γ results in the increase of the brace thickness. Three charts are given in Fig. 7, as an example, depicting the change of chord-side SCFs at the inner saddle (IS), outer saddle (OS), and crown (C) positions due to the change in the value of the τ and the interaction of this parameter with the γ under the 1st axial loading condition. Under each loading condition, a large number comparative charts were used to study the effect of the τ on the SCFs at the IS, OS, and C positions and only three of them are presented here for the sake of brevity. Results showed that under both studied loading conditions, the increase of the τ leads to the increase of SCFs at all the saddle and crown positions. This result is not dependent on the values of other geometrical parameters.

The parameter β is the ratio of brace diameter to chord diameter. Hence, the increase of the β in models having constant value of chord diameter results in the increase of brace diameter. Fig. 8 demonstrates the change of the SCFs at the IS, OS, and C positions due to the change in the value of the β and the interaction of this parameter with the α under the 1st axial loading condition. Through investigating the effect of the β on the SCFs, it can be concluded that the change of the β generally leads to the increase of the SCFs at all the saddle and crown positions. This conclusion is not dependent on either the values of other geometrical parameters or the type of axial loading.

The parameter γ is the ratio of radius to thickness of the chord. Hence, the increase of the γ in models having constant value of the chord diameter means the decrease of chord thickness. Three charts are presented in Fig. 9 depicting the change of SCFs at the IS, OS, and C positions due to the change in the value of the γ and the interaction of this parameter with the β under the 1st axial loading condition. It was observed that under both studied loading conditions, the increase of the γ results in the increase of SCFs at the saddle and crown positions.

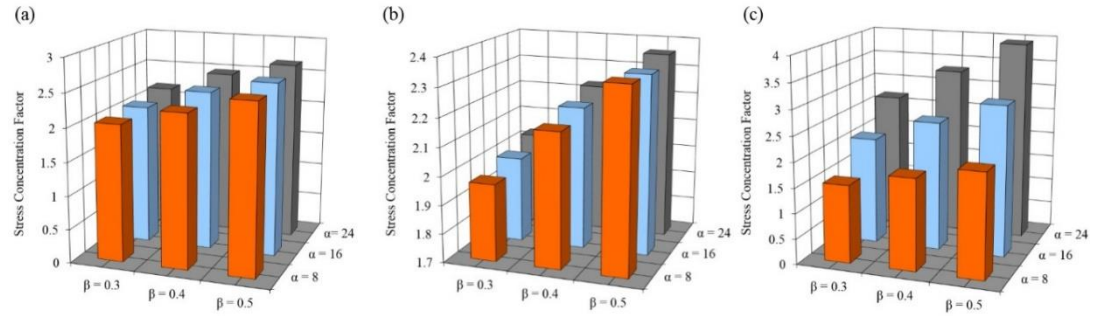

Fig. 8 The effect of the β on the SCFs at different positions ($\tau = 0.7$, $\gamma = 18$, $\eta = 0.15$; 1st axial loading condition): (a) Inner saddle, (b) Outer saddle and (c) Crown

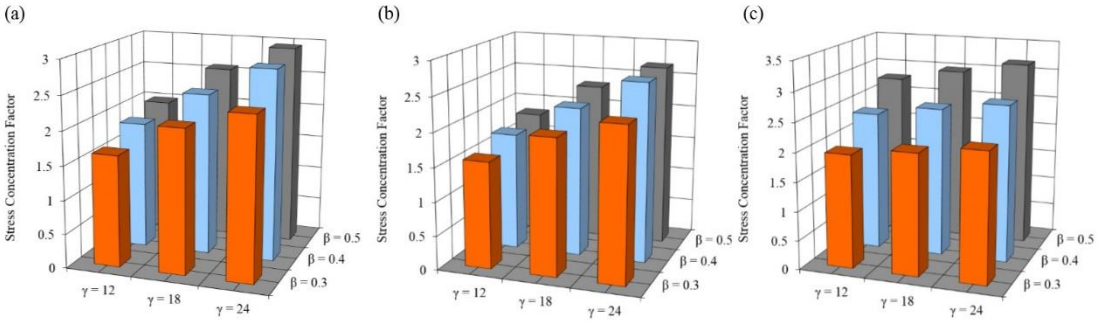

Fig. 9 The effect of the γ on the SCFs at different positions ($\alpha = 16$, $\tau = 0.7$, $\eta = 0.15$; 1st axial loading condition): (a) Inner saddle, (b) Outer saddle and (c) Crown

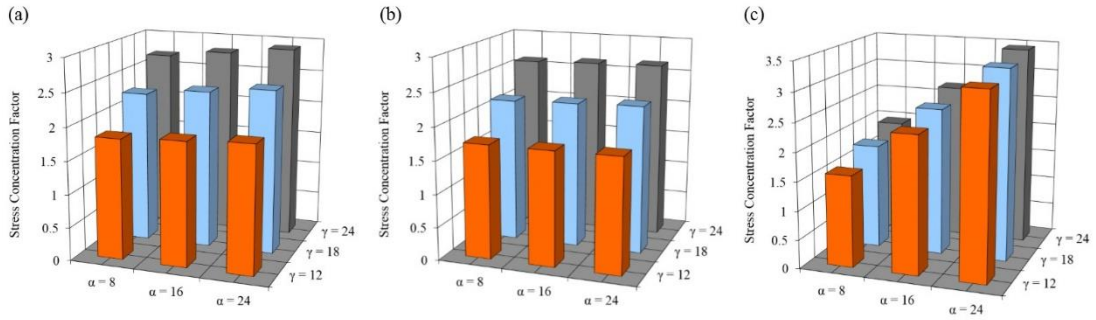

Fig. 10 The effect of the α on the SCFs at different positions ($\beta = 0.4$, $\tau = 0.7$, $\eta = 0.15$; 1st axial loading condition): (a) Inner saddle, (b) Outer saddle and (c) Crown

The parameter α is the ratio of the length to the radius of the chord. Hence, the increase of the α in models having constant value of the chord diameter means the increase of the chord length. Fig. 10 shows the change of the SCF values at the IS, OS, and C positions due to the change in the value of the α and the interaction of this parameter with the γ under the 1st axial loading condition. Results showed that the increase of the α does not have a considerable effect on the SCF values at the inner and outer saddle positions. However, at the crown position, the increase of the α leads to the increase of the SCF. These results are not dependent on either the values of other geometrical parameters or the type of axial loading.

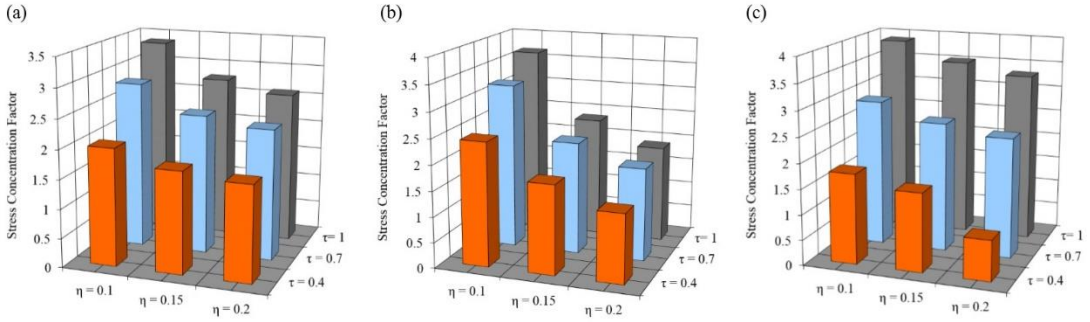

Fig. 11 The effect of the η on the SCFs at different positions (β = 0.4, α = 16, γ = 18; 1st axial loading condition): (a) Inner saddle, (b) Outer saddle and (c) Crown

Table 6 Properties of reinforced TT-joints used for the comparison of SCFs under different loading conditions

Joint ID	D (mm)	τ	β	γ	η	α	α_B
TT147	500	0.4	0.4	24	0.2	16	8
TT165	500	0.4	0.3	12	0.2	8	8
TT201	500	0.4	0.4	18	0.2	8	8
TT203	500	0.7	0.4	18	0.15	8	8
TT204	500	0.7	0.4	18	0.2	8	8
TT219	500	0.4	0.3	24	0.2	8	8

The parameter η is the ratio of the stiffener width to the chord diameter. Hence, the increase of the η in models having constant value of the chord diameter means the increase of the stiffener width. Fig. 11 shows the change of the SCF values at the IS, OS, and C positions due to the change in the value of the η and the interaction of this parameter with the τ under the 1st axial loading condition. Results showed that the increase of the η leads to the decrease of SCFs at both saddle and crown positions.

5. Effects of multi-planarity, position, and loading type on the SCFs

The uniplanar and multi-planar SCF values are compared in Fig. 12 indicating that there can be a quite big difference between the SCF values in uniplanar and two-planar T-joints. For example, under the 2nd axial loading condition, the SCF value at the outer saddle position of TT219 model (η = 0.2, β = 0.3, γ = 24, τ = 0.4) is 1.8 times the SCF at the saddle position of the corresponding uniplanar T-joint. Hence, it can be concluded that for axially loaded two-planar TT-joints, the parametric formulas of simple uniplanar T-joints are not applicable for the SCF prediction, since such formulas may lead to highly under-predicting results. Consequently, developing a set of specific parametric equations for the SCF calculation in two-planar TT-joints has practical value.

By comparing the SCFs at the considered saddle and crown positions, it can be concluded that (Fig. 12)

$$1^{st} \text{ axial loading condition:} \quad SCF_{IS} > SCF_{OS} > SCF_{C} \tag{11}$$

$$2^{nd} \text{ axial loading condition:} \quad SCF_{OS} > SCF_{IS} > SCF_{C} \tag{12}$$

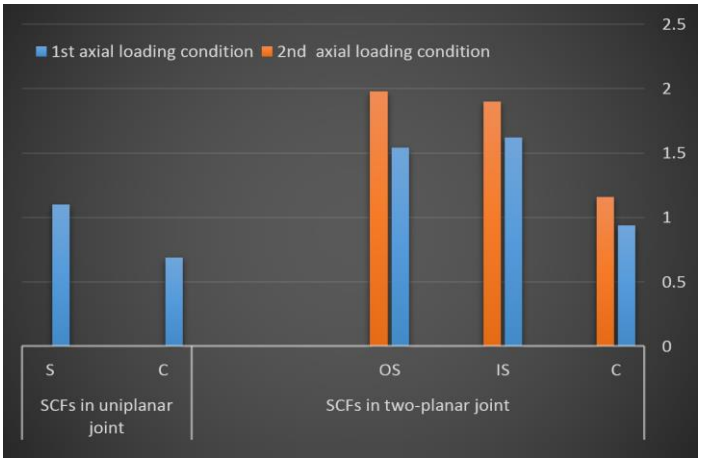

Fig. 12 Comparison of uniplanar and two-planar SCF values under the 1st and 2nd axial loading conditions

Table 7 Comparison of SCFs under the two types of axial loading condition

Joint ID	1st axial loading condition			2nd axial loading condition		
	IS	OS	C	IS	OS	C
TT147	1.92	1.76	1.51	2.19	2.34	1.64
TT165	1.12	1.05	0.77	1.40	1.47	0.96
TT201	1.63	1.5	1.04	1.90	2.05	1.25
TT203	2.28	2.17	1.81	3.52	3.66	2.44
TT204	2.13	1.79	1.63	2.41	2.76	1.94
TT219	1.62	1.54	0.94	1.90	1.98	1.16

A sample set of six two-planar TT-joints was selected (Table 6) to depict the differences among the SCFs under the two types of axial loading shown in Fig. 2. Results given in Table 7 show that the SCFs at the outer saddle position under the 2nd axial loading condition are the biggest values observed. It was also concluded that, at each considered position, the SCF under the 2nd axial loading condition is bigger than its corresponding value under the 1st axial loading condition.

6. Deriving parametric equations for the SCF calculation

Six individual parametric equations are proposed in the present paper, to calculate the SCFs at the saddle and crown positions on the weld toe of two-planar tubular TT-joints reinforced with internal ring stiffeners subjected to axial loading.

Results of multiple nonlinear regression analyses performed by SPSS were used to develop these parametric SCF design formulas. Values of dependent variable (i.e., SCF) and independent variables (i.e., β, γ, τ, α, and η) constitute the input data imported in the form of a matrix. Each row of this matrix involves the information about the SCF value at a saddle/crown position on the weld toe of an internally ring-stiffened two-planar tubular TT-joint having specific geometrical properties.

When the dependent and independent variables are defined, a model expression must be built

with defined parameters. Parameters of the model expression are unknown coefficients and exponents. The researcher must specify a starting value for each parameter, preferably as close as possible to the expected final solution. Poor starting values can result in failure to converge or in convergence on a solution that is local (rather than global) or is physically impossible. Various model expressions must be built to derive a parametric equation having a high coefficient of determination (R^2).

Following parametric equations are proposed, after performing a large number of nonlinear analyses, for the calculation of chord-side SCFs at the saddle and crown positions in two-planar tubular TT-joints reinforced with internal ring stiffeners subjected to the two considered axial loading conditions (Fig. 2):

- ***1st axial loading condition:***

Inner saddle position:

$$SCF_{1st\text{-}IS} = 0.323\,\beta^{0.309}\gamma^{0.568}\tau^{0.525}\alpha^{0.060}\eta^{-0.399};\quad R^2 = 0.953 \tag{13}$$

Outer saddle position:

$$SCF_{1st\text{-}OS} = 0.118\,\beta^{0.267}\gamma^{0.565}\tau^{0.388}\alpha^{0.009}\eta^{-0.858};\quad R^2 = 0.974 \tag{14}$$

Crown position:

$$SCF_{1st\text{-}C} = 0.548\,\beta^{0.699}\gamma^{0.153}\tau^{0.906}\alpha^{0.593}\eta^{-0.237};\quad R^2 = 0.986 \tag{15}$$

- ***2nd axial loading condition:***

Inner saddle position:

$$SCF_{2nd\text{-}IS} = 0.085\,\beta^{0.379}\gamma^{0.497}\tau^{0.532}\alpha^{0.051}\eta^{-1.399};\quad R^2 = 0.988 \tag{16}$$

Outer saddle position:

$$SCF_{2nd\text{-}OS} = 0.174\,\beta^{0.446}\gamma^{0.492}\tau^{0.624}\alpha^{0.072}\eta^{-1.093};\quad R^2 = 0.990 \tag{17}$$

Crown position:

$$SCF_{2nd\text{-}C} = 0.509\beta^{0.500}\gamma^{0.191}\tau^{0.862}\alpha^{0.401}\eta^{-0.487};\quad R^2 = 0.958 \tag{18}$$

Values obtained for R^2 are quite high indicating the accuracy of the fit. The validity ranges of dimensionless geometrical parameters for the developed equations have been given in Eq. (10).

In Fig. 13, the SCF values predicted by proposed equations are compared with the SCFs extracted from FE analyses. It can be seen that there is a good agreement between the results of proposed equations and numerically computed values.

The UK Department of Energy (DoE) (1983) recommends the following assessment criteria regarding the applicability of the commonly used SCF parametric equations (P/R stands for the ratio of the *predicted* SCF from a given equation to the *recorded* SCF from test or analysis):

- For a given dataset, if % SCFs under-predicting $\leq$ 25%, i.e. [%P/R < 1.0] $\leq$ 25%, and if % SCFs considerably under-predicting $\leq$ 5%, i.e., [%P/R < 0.8] $\leq$ 5%, then accept the equation. If, in addition, the percentage SCFs considerably over-predicting $\leq$ 50%, i.e. [%P/R > 1.5] $\geq$50%, then the equation is regarded as generally conservative.
- If the acceptance criteria is nearly met i.e. 25% < [%P/R < 1.0] $\leq$ 30%, and/or 5% < [%P/R < 0.8] $\leq$ 7.5%, then the equation is regarded as borderline and engineering judgment must be used to determine acceptance or rejection.
- Otherwise reject the equation as it is too optimistic.

In view of the fact that for a mean fit equation, there is always a large percentage of under-

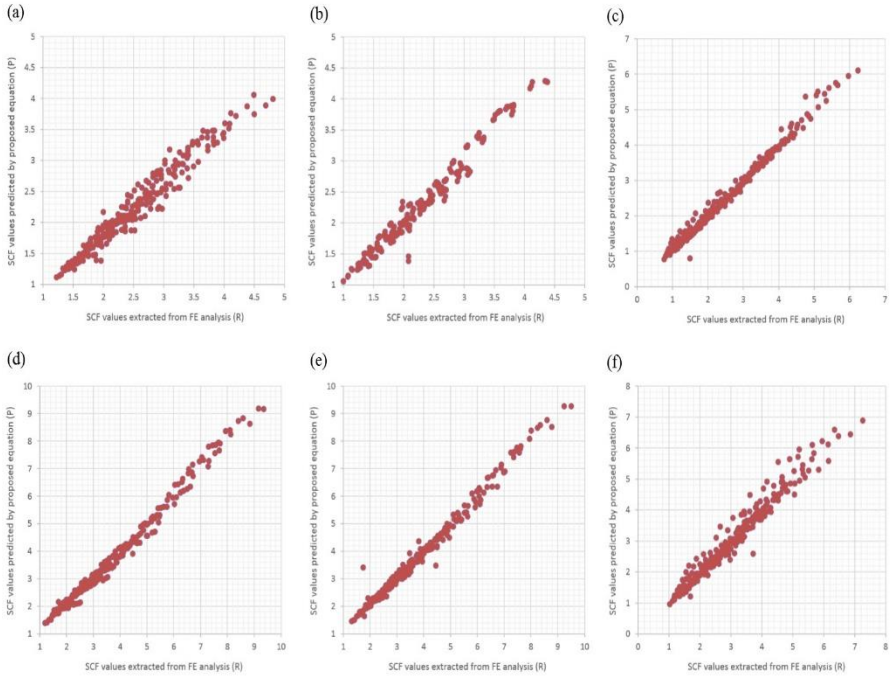

Fig. 13 Comparison of 243 SCF values calculated by the proposed equations with the corresponding SCFs extracted from the FE analysis: (a) Eq. (13), (b) Eq. (14), (c) Eq. (15), (d) Eq. (16), (e) Eq. (17), and (f) Eq. (18)

Table 8 Results of equation assessment according to the UK DoE (1983) acceptance criteria

Proposed equation	Conditions		Decision
	$\%P/R < 0.8$	$\%P/R > 1.5$	
Eq. (13)	0% < 5% OK.	0% < 50% OK.	Accept
Eq. (14)	0% < 5% OK.	0.41% < 50% OK.	Accept
Eq. (15)	2.06% < 5% OK.	0% < 50% OK.	Accept
Eq. (16)	0.41% < 5 % OK.	0% < 50% OK.	Accept
Eq. (17)	0% < 5 % OK.	0% < 50% OK.	Accept
Eq. (18)	1.65% < 5 % OK.	0% < 50% OK.	Accept

prediction, the requirement for joint under-prediction, i.e., $P/R < 1.0$, can be completely removed in the assessment of parametric equations (Bomel Consulting Engineers, 1994). Assessment results according to the UK DoE (1983) criteria are presented in Table 8 showing that all equations satisfy the criteria recommended by the UK Department of Energy.

7. Conclusions

Results of stress analyses performed on 243 FE models verified against numerical and experimental data were used to investigate the effects of geometrical parameters on the chord-side SCFs at the saddle and crown positions in two-planar tubular TT-joints, also called multi-planar DT-

joints, reinforced with internal ring stiffeners under two types of axial loading. A set of SCF parametric equations was also developed for the fatigue design. Main conclusions are summarized as follows.

The increase of the parameters τ, β, and γ leads to the increase of the SCFs at the inner saddle, outer saddle, and crown positions. The change of the α does not have a considerable effect on the SCF values at the inner and outer saddle positions. However, at the crown position, the increase of the α leads to the increase of the SCF. The increase of the η results in the decrease of the SCFs at all the considered positions.

The SCFs at the outer saddle position under the 2nd axial loading condition are the biggest values observed. It was also concluded that, at each considered position, the SCF under the 2nd axial loading condition is bigger than its corresponding value under the 1st axial loading condition.

There can be a quite big difference between the SCF values in uniplanar T- and two-planar TT-joints. Hence, for axially loaded two-planar TT-joints, the parametric formulas of simple uniplanar T-joints are not applicable for the SCF prediction, since such formulas may lead to highly under-predicting results. Consequently, developing a set of specific parametric equations for the SCF calculation in two-planar TT-joints has practical value. High coefficients of determination and the satisfaction of acceptance criteria recommended by the UK DoE guarantee the accuracy of six parametric equations proposed in the present paper. Hence, the developed equations can reliably be used for the fatigue analysis and design of internally ring-stiffened two-planar tubular TT-joints subjected to axial loading.

Acknowledgments

Useful comments of anonymous reviewers on draft version of this paper are highly appreciated.

References

Ahmadi, H. (2016), "A probability distribution model for SCFs in internally ring-stiffened tubular KT-joints of offshore structures subjected to out-of-plane bending loads", *Ocean Eng.*, **116**, 184-199, https://doi.org/10.1016/j.oceaneng.2016.02.037.

Ahmadi, H. and Kouhi, A. (2020), "Stress concentration factors of multi-planar tubular XT-joints subjected to out-of-plane bending moments", *Appl. Ocean Res.*, **96**, 102058, https://doi.org/10.1016/j.apor.2020.102058.

Ahmadi, H. and Lotfollahi-Yaghin, M.A. (2012a), "A probability distribution model for stress concentration factors in multi-planar tubular DKT-joints of steel offshore structures", *Appl. Ocean Res.*, **34**, 21-32, https://doi.org/10.1016/j.apor.2011.11.002.

Ahmadi, H. and Lotfollahi-Yaghin, M.A. (2012b), "Geometrically parametric study of central brace SCFs in offshore three-planar tubular KT-joints", *J. Constr. Steel Res.*, **71**, 149-161, https://doi.org/10.1016/j.jcsr.2011.10.024.

Ahmadi, H. and Lotfollahi-Yaghin, M.A. (2013), "Effect of SCFs on S–N based fatigue reliability of multi-planar tubular DKT-joints of offshore jacket-type structures", *Ships Offshore Struct.*, **8**, 55-72, https://doi.org/10.1080/17445302.2011.627750.

Ahmadi, H. and Lotfollahi-Yaghin, M.A. (2015), "Stress concentration due to in-plane bending (IPB) loads in ring-stiffened tubular KT-joints of offshore structures: Parametric study and design formulation", *Appl. Ocean Res.*, **51**, 54-66, https://doi.org/10.1016/j.apor.2015.02.009.

Ahmadi, H. and Mousavi Nejad Benam, M.A. (2017), "Probabilistic analysis of SCFs in unstiffened gap tubular KT-joints of jacket structures under the OPB moment loads", *Adv. Struct. Eng.*, **20**, 595-615,

https://doi.org/10.1177%2F1369433216658487.
Ahmadi, H. and Zavvar, E. (2015), "Stress concentration factors induced by out-of-plane bending loads in ring-stiffened tubular KT-joints of jacket structures", *Thin-Walled Struct.*, **91**, 82-95, https://doi.org/10.1016/j.tws.2015.02.011.
Ahmadi, H. and Zavvar, E. (2016), "The effect of multi-planarity on the SCFs in offshore tubular KT-joints subjected to in-plane and out-of-plane bending loads", *Thin-Walled Struct.*, **106**, 148-165, https://doi.org/10.1016/j.tws.2016.04.020.
Ahmadi, H., Lotfollahi-Yaghin, M.A. and Aminfar, M.H. (2011a), "Distribution of weld toe stress concentration factors on the central brace in two-planar CHS DKT-connections of steel offshore structures", *Thin-Walled Struct*., **49**, 1225-1236, https://doi.org/10.1016/j.tws.2011.06.001.
Ahmadi, H., Lotfollahi-Yaghin, M.A. and Aminfar, M.H. (2011b), "Effect of stress concentration factors on the structural integrity assessment of multi-planar offshore tubular DKT-joints based on the fracture mechanics fatigue reliability approach", *Ocean Eng.*, **38**, 1883-1893, https://doi.org/10.1016/j.oceaneng.2011.08.004.
Ahmadi, H., Lotfollahi-Yaghin, M.A. and Aminfar, M.H. (2011c), "Geometrical effect on SCF distribution in uni-planar tubular DKT-joints under axial loads", *J. Constr. Steel Res.*, **67**(8), 1282-1291, https://doi.org/10.1016/j.jcsr.2011.03.011.
Ahmadi, H., Lotfollahi-Yaghin, M.A. and Aminfar, M.H. (2012a), "The development of fatigue design formulas for the outer brace SCFs in offshore three-planar tubular KT-joints", *Thin-Walled Struct.*, **58**, 67-78, https://doi.org/10.1016/j.tws.2012.04.011.
Ahmadi, H., Lotfollahi-Yaghin, M.A. and Shao, Y.B. (2013), "Chord-side SCF distribution of central brace in internally ring-stiffened tubular KT-joints: A geometrically parametric study", *Thin-Walled Struct.*, **70**, 93-105, https://doi.org/10.1016/j.tws.2013.04.011.
Ahmadi, H., Lotfollahi-Yaghin, M.A., Shao, Y.B. and Aminfar, M.H. (2012b), "Parametric study and formulation of outer-brace geometric stress concentration factors in internally ring-stiffened tubular KT-joints of offshore structures", *Appl. Ocean Res.*, **38**, 74-91, https://doi.org/10.1016/j.apor.2012.07.004.
Ahmadi, H., Mohammadi, A.H. and Yeganeh, A. (2015), "Probability density functions of SCFs in internally ring-stiffened tubular KT-joints of offshore structures subjected to axial load", *Thin-Walled Struct.*, **94**, 485-499, https://doi.org/10.1016/j.tws.2015.05.012.
Ahmadi, H., Mohammadi, A.H., Yeganeh, A. and Zavvar, E. (2016), "Probabilistic analysis of stress concentration factors in tubular KT-joints reinforced with internal ring stiffeners under in-plane bending loads", *Thin-Walled Struct.*, **99**, 58-75, https://doi.org/10.1016/j.tws.2015.11.010.
American Petroleum Institute (API) (2007), Recommended practice for planning, designing and constructing fixed offshore platforms: Working stress design: RP 2A-WSD. 21st Edition, Errata and Supplement 3, Washington DC, US.
American Welding Society (AWS) (2002), Structural welding code: AWS D 1.1. Miami (FL), US.
Asgarian, B., Mokarram, V. and Alanjari, P. (2014), "Local joint flexibility equations for Y-T and K-type tubular joints", *Ocean Syst. Eng.*, **4**(2), 151-167, https://doi.org/10.12989/ose.2014.4.2.151.
Bomel Consulting Engineers (1994), "Assessment of SCF equations using Shell/KSEPL finite element data",
Cao, J.J., Yang, G.J. and Packer, J.A. (1997), "FE mesh generation for circular tubular joints with or without cracks", *Proceedings of the 7th International Offshore and Polar Engineering Con*ference, Honolulu (HI), US.
Chang, E. and Dover, W.D. (1999a), "Parametric equations to predict stress distributions along the intersection of tubular X and DT-joints", *Int. J. Fatigue*, **21**, 619-635, https://doi.org/10.1016/S0142-1123(99)00018-3.
Chang, E. and Dover, W.D. (1999b), "Prediction of stress distributions along the intersection of tubular Y and T-joints", *Int. J. Fatigue*, **21**, 361-381, https://doi.org/10.1016/S0142-1123(98)00083-8.
Chiew, S.P., Soh, C.K. and Wu, N.W. (1999), "Experimental and numerical stress analyses of tubular XT-joint", *J. Struct. Eng.*,**125**, 1239-1248, https://doi.org/10.1061/(ASCE)0733-9445(1999)125:11(1239).
Chiew, S.P., Soh, C.K. and Wu, N.W. (2000), "General SCF design equations for steel multiplanar tubular XX-joints", *Int. J. Fatigue*, **22**, 283–293, https://doi.org/10.1016/S0142-1123(99)00130-9.
Efthymiou, M. (1988), "Development of SCF formulae and generalized influence functions for use in fatigue

analysis", *OTJ 88*, Surrey, UK.
Gao, F. (2006), "Stress and strain concentrations of completely overlapped tubular joints under lap brace OPB load", *Thin-Walled Struct.*, **44**, 861-871, https://doi.org/10.1016/j.tws.2006.08.017.
Gao, F., Shao, Y.B. and Gho, W.M. (2007), "Stress and strain concentration factors of completely overlapped tubular joints under lap brace IPB load", *J. Constr. Steel Res.*, **63**, 305-316, https://doi.org/10.1016/j.jcsr.2006.05.007.
Gaspar, B., Garbatov, Y. and Guedes Soares, C. (2011), "Effect of weld shape imperfections on the structural hot-spot stress distribution", *Ships Offshore Struct.*, **6**(1−2), 145–159, https://doi.org/10.1080/17445302.2010.497052.
Gho, W.M. and Gao, F. (2004), "Parametric equations for stress concentration factors in completely overlapped tubular K(N)-joints", *J. Constr. Steel Res.*, **60**, 1761-1782, https://doi.org/10.1016/j.jcsr.2004.05.003.
Guarracino, F. (2011), "A simple formula for complementing FE analyses in the estimation of the effects of local conditions in circular cylindrical shells", *Comput. Model. Eng. Sci. (CMES)*, **72**(3), 167-184, doi:10.3970/cmes.2011.072.167.
Hellier, A.K., Connolly, M. and Dover, W.D. (1990), "Stress concentration factors for tubular Y and T-joints", *Int. J. Fatigue*, **12**, 13-23, https://doi.org/10.1016/0142-1123(90)90338-F.
Hoon, K.H., Wong, L.K. and Soh, A.K. (2001), "Experimental investigation of a doubler-plate reinforced tubular T-joint subjected to combined loadings", *J. Constr. Steel Res.*, **57**, 1015–1039, https://doi.org/10.1016/S0143-974X(01)00023-2.
IIW-XV-E (1999), Recommended fatigue design procedure for welded hollow section joints, IIW Docs, XV-1035-99/XIII-1804-99. International Institute of Welding, France.
Karamanos, S.A., Romeijn, A. and Wardenier, J. (1999), "Stress concentrations in multi-planar welded CHS XX-connections", *J. Constr. Steel Res.*, **50**, 259-282, https://doi.org/10.1016/S0143-974X(98)00244-2.
Karamanos, S.A., Romeijn, A. and Wardenier, J. (2000), "Stress concentrations in tubular gap K-joints: mechanics and fatigue design", *Eng. Struct.*, **22**, 4-14, https://doi.org/10.1016/S0141-0296(98)00062-5.
Karamanos, S.A., Romeijn, A. and Wardenier, J. (2002), "SCF equations in multi-planar welded tubular DT-joints including bending effects", *Mar. Struct.*, **15**, 157-173, https://doi.org/10.1016/S0951-8339(01)00020-X.
Kuang, J.G., Potvin, A.B. and Leick, R.D. (1975), "Stress concentration in tubular joints", *Proceedings of the Offshore Technology Conference*, Paper OTC 2205, Houston (TX), US.
Lee, M.K. and Wilmshurst, S.R. (1995), "Numerical modeling of CHS joints with multiplanar double-K configuration", *J. Constr. Steel Res.*, **32**, 281-301, https://doi.org/10.1016/0143-974X(95)93899-F.
Lee, M.M.K. (1999), "Strength, stress and fracture analyses of offshore tubular joints using finite elements", *J. Constr. Steel Res.*, **51**, 265-286, https://doi.org/10.1016/S0143-974X(99)00025-5.
Liu, G., Zhao, X. and Huang, Y. (2015), "Prediction of stress distribution along the intersection of tubular T-joints by a novel structural stress approach", *Int. J. Fatigue*, **80**, 216-230, https://doi.org/10.1016/j.ijfatigue.2015.05.021.
Lotfollahi-Yaghin, M.A. and Ahmadi, H. (2010), "Effect of geometrical parameters on SCF distribution along the weld toe of tubular KT-joints under balanced axial loads", *Int. J. Fatigue*, **32**, 703-719, https://doi.org/10.1016/j.ijfatigue.2009.10.008.
Lotfollahi-Yaghin, M.A. and Ahmadi, H. (2011), "Geometric stress distribution along the weld toe of the outer brace in two-planar tubular DKT-joints: parametric study and deriving the SCF design equations", *Mar. Struct.*, **24**, 239-260, https://doi.org/10.1016/j.marstruc.2011.02.005.
Morgan, M.R. and Lee, M.M.K. (1998a), "Parametric equations for distributions of stress concentration factors in tubular K-joints under out-of-plane moment loading", *Int. J. Fatigue*, **20**, 449-461, https://doi.org/10.1016/S0142-1123(98)00011-5.
Morgan, M.R. and Lee, M.M.K. (1998b), "Prediction of stress concentrations and degrees of bending in axially loaded tubular K-joints", *J. Constr. Steel Res.*, **45**(1), 67-97, https://doi.org/10.1016/S0143-974X(97)00059-X.
Myers, P.T., Brennan, F.P. and Dover, W.D. (2001), "The effect of rack/rib plate on the stress concentration factors in jack-up chords", *Mar. Struct.*, **14**, 485-505, https://doi.org/10.1016/S0951-8339(00)00051-4.

N'Diaye, A., Hariri, S., Pluvinage, G. and Azari, Z. (2007), "Stress concentration factor analysis for notched welded tubular T-joints", *Int. J. Fatigue*, **29**, 1554-1570, https://doi.org/10.1016/j.ijfatigue.2006.10.030.

Nwosu, D.I., Swamidas, A.S.J. and Munaswamy, K. (1995), "Numerical stress analysis of internal ring-stiffened tubular T-joints", *J. Offshore Mech. Arct.*, **117**, 113-125, https://doi.org/10.1115/1.2827061.

Prashob, P.S., Shashikala, A.P. and Somasundaran, T.P. (2018), "Effect of FRP parameters in strengthening the tubular joint for offshore structures", *Ocean Syst. Eng.*, **8**(4), 409-426, https://doi.org/10.12989/ose.2018.8.4.409.

Shao, Y.B. (2004a), "Fatigue behaviour of uni-planar CHS gap K-joints under axial and in-plane bending loads", Ph.D. Dissertation, School of Civil & Environmental Engineering, Nanyang Technological University, Singapore.

Shao, Y.B. (2004b), "Proposed equations of stress concentration factor (SCF) for gap tubular K-joints subjected to bending load", *Int. J. Space Struct.*, **19**, 137-147, https://doi.org/10.1260%2F0266351042886667.

Shao, Y.B. (2007), "Geometrical effect on the stress distribution along weld toe for tubular T- and K-joints under axial loading", *J. Constr. Steel Res.*, **63**, 1351-1360, https://doi.org/10.1016/j.jcsr.2006.12.005.

Shao, Y.B., Du, Z.F. and Lie, S.T. (2009), "Prediction of hot spot stress distribution for tubular K-joints under basic loadings", *J. Constr. Steel Res.*, **65**, 2011-2026, https://doi.org/10.1016/j.jcsr.2009.05.004.

Smedley, P. and Fisher, P. (1991), "Stress concentration factors for simple tubular joints", *Proceedings of the International Offshore and Polar Engineering Conference (ISOPE)*, Edinburgh.

Swanson Analysis Systems Inc. (2009), "ANSYS contact technology guide", Canonsburg (PA), US.

UK Department of Energy (DoE) (1983), "Background notes to the fatigue guidance of offshore tubular joints", UK DoE, London, UK.

UK Health and Safety Executive (1995), "Offshore installations: guidance on design, construction and certification", 3rd amendment to 4th edition. London, UK.

UK Health and Safety Executive (HSE) (1997), "OTH 354: Stress concentration factors for simple tubular joints − assessment of existing and development of new parametric formulae", UK HSE, London, UK.

Wimpey Offshore (1991), "In-service database for ring-stiffened tubular joints", Report WOL 035/91.

Wingerde, A.M., Packer, J.A. and Wardenier, J. (2001), "Simplified SCF formulae and graphs for CHS and RHS K- and KK-connections", *J. Constr. Steel Res.*, **57**, 221-252, https://doi.org/10.1016/S0143-974X(00)00015-8.

Woghiren, C.O. and Brennan, F.P. (2009), "Weld toe stress concentrations in multi planar stiffened tubular KK Joints", *Int. J. Fatigue*, **31**, 164-172, https://doi.org/10.1016/j.ijfatigue.2008.03.039.

Xu, F., Chen, J. and Jin, W. (2015), "Experimental investigation of SCF distribution for thin-walled concrete-filled CHS joints under axial tension loading", *Thin-Walled Struct.*, **93**, 149-157, https://doi.org/10.1016/j.tws.2015.03.019.

Yang, J., Chen, Y. and Hu, K. (2015), "Stress concentration factors of negative large eccentricity tubular N-joints under axial compressive loading in vertical brace", *Thin-Walled Struct.*, **96**, 359-371, https://doi.org/10.1016/j.tws.2015.08.027.

PL